

Infrared Spectra of Molecules and Materials  
of Astrophysical Interest

Grant NGL-41-002-003  
Quarterly Progress Report  
Report Number 32  
July 1975

(NASA-CR-143025) INFRARED SPECTRA OF  
MOLECULES AND MATERIALS OF ASTROPHYSICAL  
INTEREST Quarterly Progress Report, 15 Mar.  
- 15 Jun. 1975 (South Carolina Univ.) 55 p  
HC \$4.25

N75-26950

Unclas  
26641

CSSL 03B G3/90

Office of Grants and Research Contracts  
Office of Space Science and Applications  
National Aeronautics and Space Administration  
Washington, D. C. 20546

(Prepared under Grant NGL-41-002-003 by the  
University of South Carolina, Columbia, South Carolina, 29208)



Principal Investigator: James R. Durig, Professor of Chemistry  
Period Covered: 15 March 1975 to 15 June 1975

## SUMMARY OF PROGRESS

We have been studying the vibrational spectra from 4000 to  $33\text{ cm}^{-1}$  of several molecules which may be present in the atmosphere of the Jovian planets. These studies have been made to provide vibrational frequencies which can be used to: (1) determine the composition of the cloud covers of several of the planets, (2) provide structural information under favorable circumstances, (3) provide necessary data from which accurate thermodynamic data can be calculated, and (4) furnish information as to the nature of the potential energy function of the molecules and forces acting within them.

Some of the molecules which we have studied can be produced photochemically from methane, ammonia, and hydrogen sulfide which are thought to be constituents of the planets with reducing atmospheres. Some of the compounds will polymerize under ultraviolet radiation and drop out of the atmospheres. However, planets with a hot base, like that of Jupiter, may rebuild molecules destroyed photochemically. Therefore, we have used these criteria in selecting the compounds which we have studied.

Gerald P. Kuiper<sup>1</sup> has pointed out that the Jovian atmosphere is expected to contain  $\text{H}_2$ , He,  $\text{N}_2$ ,  $\text{H}_2\text{O}$ ,  $\text{NH}_3$ ,  $\text{CH}_3$ , Ar, and possibly  $\text{SiH}_4$ . He has also listed a number of other gases that should be considered because they are composed of fairly abundant atomic species and have boiling points below  $120^\circ\text{C}$  (see Table 8, pg. 349-350 of reference 1). He has also pointed out that until more is known about the atmospheres of the planets, it is useful to keep a fairly large number of possible constituents in mind in planning further spectroscopic work.

In our initial work on the vibrational spectra of molecules of astrophysical interest, we studied hydrazine,<sup>2</sup> methylamine,<sup>3</sup> as well as several substituted hydrazines.<sup>4-8</sup> Recently both ethane and acetylene have been

found in the atmosphere of Jupiter.<sup>9</sup> It is expected that substituted ethanes will also be eventually found in some of the planetary atmospheres. In fact, ethanol has been found in the Sagittarius B2 cloud of dust and gas which is near the center of the Milky Way.<sup>10</sup> In addition, molecules such as acetaldehyde ( $\text{CH}_3\text{CHO}$ ), methanol ( $\text{CH}_3\text{OH}$ ), dimethylether ( $\text{CH}_3)_2\text{O}$ , formic acid ( $\text{HCOOH}$ ), have been identified in outer space. Additionally, there is a good chance that glyoxal ( $\text{CHOCHO}$ ) may be found as a molecule in outer space. As a continuation of our earlier studies<sup>11, 12</sup> on this molecule, we have undertaken an investigation of the Raman and infrared spectra of solid glyoxal- $\text{d}_1$  and glyoxal- $\text{d}_2$  and we should like to report our results herein. The infrared<sup>13</sup> and electronic<sup>14-17</sup> spectra of trans-glyoxal(I) and its deuterated analogs in the vapor state have been very thoroughly studied. The vapor state Raman data have not yet been recorded except for the  $\nu_1$  transition of  $\text{C}_2\text{H}_2\text{O}_2$  at  $2843\text{ cm}^{-1}$  observed by Holzer and Ramsay<sup>17</sup> with an argon-ion laser. Because of absorption and fluorescence in the blue-green region of the spectrum, it is necessary to use a red laser such as He-Ne for best observation of the Raman spectrum, and Verderame, Castellucci, and Califano<sup>18</sup> and Durig and Hannum<sup>11</sup> have studied the Raman spectrum of solid  $\text{C}_2\text{H}_2\text{O}_2$  at low temperatures in this manner. They combined these measurements with observations of the infrared spectrum, assigned the frequencies to normal modes and showed that the rule of mutual exclusion holds well in the crystalline state. Although some discrepancies exist between the frequencies measured by Verderame, Castellucci, and Califano and those by Durig and Hannum the assignments are not in doubt. Le Khyu Kho and Tyulin<sup>19</sup> have made similar measurements on liquid  $\text{C}_2\text{H}_2\text{O}_2$ .

The present study extends this work to solid glyoxal- $\text{d}_1$  and glyoxal- $\text{d}_2$ . These compounds are of interest since the loss of the center of symmetry in the monodeutero compound ( $\text{C}_s$ ) means that coincidences will occur in the Raman- and infrared-active modes, whereas glyoxal- $\text{d}_2$  ( $\text{C}_{2h}$ ) should exhibit rigorous mutual

exclusion. Also, there has been some interest in  $\nu_4$ , the C-C stretching frequency in these molecules<sup>20</sup> and the Raman spectrum is expected to give clear evidence on this mode.

The results of this study have been submitted for publication in the Journal of Raman Spectroscopy and a copy of the complete paper is given in Appendix I. The results and discussion from this paper follow:

a. Glyoxal- $d_2$

The infrared and Raman spectra of dideuteroxyglyoxal are analogous in most respects to those of  $C_2H_2O_2$ . They clearly demonstrate the  $C_{2h}$  molecular symmetry of the trans molecules and  $C_i(T)$  site symmetry in the crystal since six fundamentals ( $2A_u + 4B_u$ ) appear strongly in the infrared spectrum and 6 ( $5A_g + B_g$ ) in the Raman spectrum. Admittedly, there is a possible very slight breakdown of the rule of mutual exclusion due to the polycrystalline environment of the molecules since a very weak infrared shoulder occurs at about  $1703\text{ cm}^{-1}$  [ $\nu_2(A_g) = 1709\text{ cm}^{-1}$ ] on the side of the very intense  $\nu_{10}$  band, and an extremely weak Raman line at  $1681\text{ cm}^{-1}$  [ $\nu_{10}(B_u) = 1685\text{ cm}^{-1}$ ], but none of the other fundamentals are found in either spectrum in violation of the  $C_{2h}$  selection rules.

The observed frequencies are easily assigned to normal modes by comparison with the vapor data and an examination of the data reveals that, as for  $C_2H_2O_2$ , all vibration frequencies are higher in the solid than the vapor, with the exception of the two carbonyl frequencies and, marginally,  $\nu_8$  the CD wagging mode. Some of the displacements from the vapor to the solid are quite large, e.g., +31 and +47  $\text{cm}^{-1}$  for the CH stretching modes, +32 for the in-plane skeletal band,  $\nu_{12}$ , +56  $\text{cm}^{-1}$  for the torsion, and -13 and -29  $\text{cm}^{-1}$  for the two carbonyl stretching modes. The shift in the torsion amounts to nearly 50% of the vapor frequency and an equally large change was noted for  $C_2H_2O_2$ <sup>11,18</sup>. This obviously is the result of very strong intermolecular interactions in the

crystal. Dideuterglyoxal does show some weak absorption at  $121\text{ cm}^{-1}$  (vapor torsion =  $118\text{ cm}^{-1}$ ), but we prefer to assign the very intense band at  $174\text{ cm}^{-1}$  to the torsion and that at  $121\text{ cm}^{-1}$  to a lattice mode.

As found for  $\text{C}_2\text{H}_2\text{O}_2$  only the C-D in-plane rocking band at  $1019, 1025\text{ cm}^{-1}$  exhibits factor group splitting, indicating that there must be at least two molecules per primitive unit cell. However, the absence of other such effects shows that vibrational coupling between molecules within the cell is not large.

The C-C stretching mode,  $\nu_4$ , appears clearly in the Raman spectrum at  $944\text{ cm}^{-1}$  (cf.  $1078\text{ cm}^{-1}$  for glyoxal). A number of weak bands in the infrared spectrum are assigned to binary combinations of one infrared-active mode and one Raman-active mode as indicated in Table I of Appendix I. No first overtones are allowed by the  $\text{C}_{2h}$  symmetry although  $2\nu_{10}$  appears weakly. The combination band,  $\nu_3 + \nu_{11}$  ( $\text{B}_u$ ) at  $1231\text{ cm}^{-1}$  is relatively intense and must be considered as a component of a Fermi doublet with  $\nu_9$  ( $\text{B}_u$ ) at  $2177\text{ cm}^{-1}$ . One overtone,  $2\nu_5$ , occurs in the Raman spectrum.

#### b. Glyoxal- $\text{d}_1$

This compound gives a classical example of the breakdown of the principle of mutual exclusion on loss of the center of symmetry by partial deuteration. All twelve modes of  $\text{C}_2\text{HDO}_2$  ( $\text{C}_s$ ) can be both infrared- and Raman-active, but although the center of symmetry has gone, the overall degree of asymmetry of the molecule is low, so that some transition probabilities will remain low. However, eight clear coincidences are observed. In the cases of  $\text{C}_2\text{H}_2\text{O}_2$  and  $\text{C}_2\text{D}_2\text{O}_2$ , the symmetrical carbonyl stretching vibration,  $\nu_2$ , is Raman-active and the antisymmetrical mode,  $\nu_{10}$ , is infrared-active. In  $\text{C}_2\text{HDO}_2$  both transitions occur in both types of spectra, but  $\nu_2$  is very much the stronger in the Raman effect, and  $\nu_{10}$  very much the stronger in the infrared spectrum.

The clear coincidences occur at 2882, 2161, 1720, 1699, 1352, 1116, 1005, and  $981\text{ cm}^{-1}$  which are readily assigned to the CH stretch, CD stretch, symmetrical CO stretch, antisymmetrical CO stretch, CH rock, CC stretch, CH out-of-plane wag, and CD rock, respectively. In general, the agreement between the infrared and Raman frequencies is well within the accuracy of the instruments, but a small anomaly is noticed in the case of the symmetrical carbonyl stretch,  $\nu_2$ , where the infrared maximum occurs at  $1725\text{ cm}^{-1}$  and the Raman at  $1720\text{ cm}^{-1}$ . This discrepancy could be due to slight differences in the degree of crystallinity of the different solid samples, which were difficult to anneal because of high volatility.

The remaining fundamentals are easily identified at  $548\text{ cm}^{-1}$  (C-C=O symmetrical bend) in the Raman spectrum, and at  $710\text{ cm}^{-1}$  (CD out-of-plane wag),  $357\text{ cm}^{-1}$  (antisymmetric C-C=O bend) and  $193\text{ cm}^{-1}$  (torsion) in the infrared spectrum. It is interesting to note that three of these four fundamentals, for which the change of a hydrogen atom for a deuterium is insufficient to violate the  $C_{2h}$  selection rules, all involve principally motion only of the O=C-C=O skeleton.

Cole and Osborne<sup>13</sup> were unable to detect  $\nu_6$ , the C-D out-of-plane wag in the infrared spectra of  $C_2HDO_2$  and  $C_2D_2O_2$  vapor, although product rule calculations indicated that they would lie near  $688\text{ cm}^{-1}$  and  $630\text{ cm}^{-1}$ , respectively. In the infrared spectra of the solids they are found at  $710\text{ cm}^{-1}$  and  $643\text{ cm}^{-1}$ .

The C-C stretching mode,  $\nu_4$ , is clearly indicated at about  $1116\text{ cm}^{-1}$  in both the Raman and infrared spectra. This frequency has been somewhat difficult to identify in the infrared spectrum of the vapor due to lack of resolvable rotational fine structure in the weak band found by Cole and Osborne<sup>13</sup>. It had been predicted to lie near  $1104\text{ cm}^{-1}$  on the basis of normal coordinate calculations by Fukuyama, Kuchitsu, and Morino (see Ref. 13) and ..

was found at that frequency in the laser-excited emission spectrum of the vapor<sup>19</sup>.

The infrared band due to  $\nu_{11}$ , the in-plane CH rocking mode, is not subject to factor group splitting in contrast to the analogous bands of  $C_2H_2O_2$  and  $C_2D_2O_2$  mentioned above. This is an obvious consequence of the loss of symmetry in the monodeutero compound.

A comparison of the frequencies of the solid and the vapor shows that monodeuterglyoxal parallels the behavior of glyoxal. Only the carbonyl stretching modes move to lower frequency on crystallization. Again, the torsional mode is drastically increased in frequency, this time to  $193\text{ cm}^{-1}$  (cf. vapor  $123\text{ cm}^{-1}$ ). Weak infrared absorption is found at 122, 133, and  $138\text{ cm}^{-1}$  but these are attributed to lattice modes.

First overtones and combinations are both allowed in the infrared spectrum of  $C_2HDO_2$  and a number have been assigned (Table II of Appendix I). In particular, it should be noted that all three combination modes,  $2\nu_2$ ,  $\nu_2 + \nu_{10}$ , and  $2\nu_{10}$ , involving the carbonyl stretching modes are observed.

Table III of Appendix I summarizes the vapor and solid data for the three trans-glyoxals.

Finally, it should be noted that at the low sample temperatures used in the present work, no Raman lines or infrared bands attributable to cis-glyoxal<sup>12, 21-22</sup> could be detected.

Closely related to our studies on nitrogen-containing compounds is our work on the corresponding phosphines. Phosphine itself is a molecule which has a high probability of being found in a planetary atmosphere. Additionally, for reducing-atmospheres, there is a possibility of silane being present. Because of the ultraviolet radiation, some of these molecules could be formed photochemically and silylphosphine is such a molecule. Therefore, we have turned our attention to a study of the microwave and Raman spectra,

dipole moment, barrier to internal rotation, and vibrational assignment of silylphosphine. We have been interested<sup>23</sup> for some time in the magnitude of the barriers to internal rotation around single bonds. Much of the reliable data now available on barrier heights is for C-C or C-X (where X = Si, Ge, N, P, O, S) bonds and there is little information available on the barriers to internal rotation around Si-X (where X = N, P, O, S) bonds. As part of a broad program to evaluate such barriers we recorded<sup>24</sup> the microwave spectrum of silylphosphine but during the course of our work a preliminary study of the microwave spectrum of this molecule was reported.<sup>25</sup> However, there have been no reported microwave or vibrational studies of silylphosphine-d<sub>2</sub>.

Linton and Nixon<sup>26</sup> reported the infrared (300-4000 cm<sup>-1</sup>) spectrum in the gas phase of silylphosphine and suggested that the overtone of the torsion was in the 480 cm<sup>-1</sup> range. Additionally, these authors<sup>26</sup> assigned six of the remaining fourteen fundamentals positively and a further seven tentatively but pointed out that the spectra of several deuterated species would be quite valuable in assessing the correctness of their assignments. More recently, Drake and Riddle<sup>27</sup> reported the infrared spectrum of gaseous SiD<sub>3</sub>PD<sub>2</sub> and carried out a normal coordinate calculation for both the "light" and totally deuterated species. On the bases of these studies, these authors<sup>27</sup> reassigned the deformational motions for the "light" compound. However, they<sup>27</sup> stressed that the exact geometry of the silylphosphine is unknown so that their results could be subject to considerable error on this point alone. Additionally, their data was limited to above 400 cm<sup>-1</sup> so that no information was obtained on the internal torsional mode. There have been no published Raman data on any of the isotopic species of silylphosphine. Thus, we have recorded the Raman spectra of silylphosphine in the gaseous, liquid, and solid states and the Raman spectrum of silylphosphine-d<sub>2</sub> in the gaseous state to provide additional data for making vibrational assignments



for the normal modes. The results for this study can be summarized by the following abstract:

Abstract. The microwave spectrum of  $\text{SiH}_3\text{PD}_2$  have been recorded in the range 26.5 to 40.0 GHz. Both a- and c-type transitions were observed and assigned. The rigid rotor rotational constants were determined to be:  $A = 37589.06 \pm 0.11$ ,  $B = 5315.70 \pm 0.02$ , and  $C = 5258.70 \pm 0.02$  MHz. The barrier to internal rotation has been calculated from the A-E splittings to be  $1512 \pm 26$  cal/mole. The dipole moment components of  $|\mu_a| = 0.22 \pm 0.01$ ,  $|\mu_c| = 0.56 \pm 0.01$ , and  $|\mu_t| = 0.60 \pm 0.01$  D were determined from the Stark effect. By using previously determined microwave data for  $\text{SiH}_3\text{PH}_2$ , several structural parameters have been calculated and their values are compared to similar ones in other compounds. The Raman ( $0\text{--}2500\text{ cm}^{-1}$ ) spectra of gaseous, liquid, and solid  $\text{SiH}_3\text{PH}_2$  and gaseous  $\text{SiH}_3\text{PD}_2$  have been recorded and interpreted in detail on the basis of  $C_s$  molecular symmetry.

These experimental results have been submitted for publication in the Journal of Molecular Spectroscopy and a copy of the complete paper is given as Appendix II to this report.

#### FUTURE WORK

We are continuing the studies of glyoxal and we have completed the microwave investigation of glyoxal- $\text{d}_1$  and glyoxal- $\text{d}_2$ . We shall report our findings on this part of our study in the next progress report. With these data we should be able to determine the structure of this molecule and better characterize the potential function with the additional data on the cis conformer.

Studies are also nearly complete on  $(\text{CH}_3)_2\text{NH}$  and on methylchloroformate. We are working on a computer program for the interpretation of the torsional data on  $(\text{CH}_3)_2\text{NH}$ . Also currently in progress, is a vibrational study of

$C_2H_5CN$ . We shall also continue our current work on several solutes which have potential interest as planetary atmosphere materials. In particular, we want to complete our studies of the NO dimer and we expect to have this work as part of our next progress report as well.

## REFERENCES

1. G. P. Kuiper, Atmospheres of the Earth and Planets, University of Chicago Press, Chicago, 1952.
2. J. R. Durig, S. F. Bush, and E. E. Mercer, J. Chem. Phys., 44, 4238 (1966).
3. J. R. Durig, S. F. Bush, and F. G. Baglin, J. Chem. Phys., 49, 2106 (1968).
4. J. R. Durig, W. C. Harris, and D. W. Wertz, J. Chem. Phys., 50, 1449 (1969).
5. J. R. Durig and W. C. Harris, J. Chem. Phys., 51, 4457 (1969).
6. J. R. Durig and W. C. Harris, J. Chem. Phys., 55, 1735 (1971).
7. J. R. Durig, R. W. MacNamee, L. B. Knight, and W. C. Harris, Inorg. Chem., 12, 804 (1973).
8. J. R. Durig, J. W. Thompson, and J. D. Witt, Inorg. Chem., 11, 2477 (1972).
9. Chem. Eng. News., 4, 4 (1974).
10. Ind. Res., May 1974, page 29, by Nat. Radio Astronomy Observatory at Kitt Peak.
11. J. R. Durig, and S. E. Hannum, J. Cryst. Mol. Struct., 1, 131 (1971).
12. J. R. Durig, C. C. Tong, and Y. S. Li, J. Chem. Phys., 57, 4425 (1972).
13. A. R. H. Cole, and G. A. Osborne, Spectrochim. Acta, 27A, 2461 (1971).
14. J. Paldus and D. A. Ramsay, Can. J. Phys., 45, 1389 (1967).
15. F. W. Birss, J. M. Brown, A. R. H. Cole, A. Lofthus, S. L. N. G. Krishnamachari, G. A. Osborne, J. Paldus, D. A. Ramsay, and L. Watmann, Can. J. Phys., 48, 1230 (1970).
16. D. M. Agar, E. J. Bair, F. W. Birss, P. Borrell, P. C. Chen, G. N. Currie, A. J. McHugh, B. J. Orr, D. A. Ramsay, and J. Y. Roncin, Can. J. Phys., 49, 323 (1971).
17. W. Holzer, and D. A. Ramsay, Can. J. Phys., 48, 1759 (1970).
18. F. D. Verderame, E. Castellucci, and S. Califano, J. Chem. Phys., 52, 719 (1970).
19. L. K. Kho, and V. I. Tyulin, Opt. Spektrosk., 35, 770 (1973).
20. R. Y. Dong and D. A. Ramsay, Can. J. Phys., 51, 1491 (1973).
21. G. W. Currie and D. A. Ramsay, Can. J. Phys., 49, 317 (1971).
22. D. A. Ramsay and C. Zauli, Acta Phys. Acad. Sci. Hung., 35, 79 (1974).
23. J. R. Durig, S. M. Craven, and W. C. Harris, in Vibrational Spectra and Structure, Vol. I, (J. R. Durig, ed.), Marcel Dekker, New York, 1972, p. 73.

24. M. M. Chen, M. S. Thesis, Univ. of South Carolina, Columbia, South Carolina, 1972.
25. R. Varma and K. R. Ramaprasad, 4th Austin Symposium on Gas Phase Molecular Structure, Austin, Texas, 1972. Paper T5; K. R. Ramaprasad, Ph. D. Thesis, New York Univ., 1972.
26. H. R. Linton and E. R. Nixon, Spectrochim. Acta, 11, 146 (1959).
27. J. E. Drake and C. Riddle, Spectrochim. Acta, 26A, 1697 (1970).

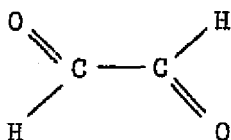
## APPENDIX I

### RAMAN AND INFRARED SPECTRA OF SOLID GLYOXAL- $d_1$ AND GLYOXAL- $d_2$

ABSTRACT. The Raman spectra of solid glyoxal- $d_1$  and glyoxal- $d_2$  have been recorded at  $-190^{\circ}\text{C}$  from 100 to  $3000\text{ cm}^{-1}$ . Fundamental frequencies of glyoxal- $d_2$  were observed at 2169, 1709, 1131, 944, 908 and  $543\text{ cm}^{-1}$  and assigned as the C-D stretching, C=O stretching, C-D rocking, C-C stretching, C-D wagging and C-C=O bending modes respectively. The infrared spectra of the solids have been recorded from 90 to  $4000\text{ cm}^{-1}$ . For  $\text{C}_2\text{D}_2\text{O}_2$  this gives the other six fundamentals at 2177, 1685, 1022, 643, 343 and  $174\text{ cm}^{-1}$ . The rule of mutual exclusion holds rigorously showing that the molecule has a centrosymmetric structure in the crystal and that the site is  $\text{C}_i(\bar{1})$ . The Raman and infrared spectra of glyoxal- $d_1$  show many coincidences, confirming the breakdown of the rule of mutual exclusion when the center of symmetry is lost on partial deuteration. Fundamentals are assigned at 2882, 2161, 1720, 1699, 1352, 1116, 1005, 981, 710, 548, 357 and  $193\text{ cm}^{-1}$ . The frequency shifts upon solidification are discussed.

## 1. Introduction

The infrared [1] and electronic [2-5] spectra of trans-glyoxal (I) and its deuterated analogs in the vapor state have



I

been very thoroughly studied, but vapor state Raman data have not yet been reported except for the  $\nu_1$  transition of  $C_2H_2O_2$  at  $2843\text{ cm}^{-1}$  observed by Holzer and Ramsay [5] with an argon ion laser.

Because of absorption and fluorescence in the blue-green region of the spectrum, it is necessary to use a red laser such as He-Ne for best observation of the Raman spectrum, and Verderame, Castellucci and Califano [6] and Durig and Hannum [7] have studied the Raman spectrum of solid  $C_2H_2O_2$  at low temperatures in this manner. They combined these measurements with observations of the infrared spectrum, assigned the frequencies to normal modes and showed that the rule of mutual exclusion holds well in the crystalline state. Although some discrepancies exist between the frequencies measured by Verderame, Castellucci and Califano and those by Durig and Hannum the assignments are not in doubt. Le Khyu Kho and Tyulin [8] have made similar measurements on liquid  $C_2H_2O_2$ .

The present paper extends this work to solid glyoxal- $d_1$  and glyoxal- $d_2$ . These compounds are of interest since the loss of

the center of symmetry in the monodeutero-compound ( $C_s$ ) means that coincidences will occur in the Raman- and infrared-active modes, while glyoxal- $d_2$  ( $C_{2h}$ ) should exhibit rigorous mutual exclusion. Also, there has been some interest in  $\nu_4$ , the C-C stretching frequency in these molecules [9] and the Raman spectrum is expected to give clear evidence on this mode.

## 2. Experimental

The deuterated glyoxals were prepared by oxidizing 1,1-dideuteroethylene (for  $C_2HDO_2$ ) and tetradeuteroethylene (for  $C_2D_2O_2$ ) with a mixture of selenium dioxide and phosphorus pentoxide in a vacuum line [10]. After drying by passage through phosphorus pentoxide the product was collected in a dry-ice-acetone trap and purified by trap-to-trap distillation. Each product was stored as the solid at  $-78^\circ C$ , at which temperature little polarization occurred.

The Raman spectra were recorded on a Cary Model 82 spectrometer equipped with a Spectra-Physics Model 125 He-Ne laser giving about 40 mW at the sample. The instrument was calibrated with emission lines of neon. For Raman measurements at  $-190^\circ C$  the samples were sublimed on to the end of the cold metal block in a Raman cell similar to that used by Durig, Riethmiller and Li [11]. The Raman spectra, measured at  $90^\circ$  to the incident radiation, are presented in Figs. 1 and 4, and the observed frequencies are listed in Tables I and II.

The mid-infrared spectra were recorded on a Perkin Elmer Model 621 spectrometer, purged with dry nitrogen, and calibrated with standard gases [12]. Monodeuterglyoxal was studied in a conventional cell cooled with liquid nitrogen, while for dideutero-glyoxal a Cryogenic Technology, Inc., cryogenic cell was employed. The

samples were deposited from the vapor on to CsI substrates which could be rotated  $90^\circ$  with respect to the light beam, and annealed before spectra were recorded. Typical spectra are shown in Figs. 2 and 5 and the observed frequencies are given in Tables I and II.

Far infrared spectra from 90 to  $300\text{ cm}^{-1}$  were obtained with a Beckman Model IR11 spectrometer which was purged with dry nitrogen and calibrated with the water vapor pure rotational spectrum [13]. The samples were condensed on a wedged silicon window in a cooled cell similar to that described by Baglin, Bush and Durig [14] and typical spectra are shown in Figs. 3 and 6. Some slight difficulty was experienced in controlling the sample thickness of  $\text{C}_2\text{D}_2\text{O}_2$  during the deposition and annealing.

After Raman and infrared spectra had been recorded the samples were sublimed off the substrate and no residual scattering or absorption respectively, which could be attributed to polymer, remained.

### 3. Results and Discussion

#### (a) Glyoxal- $\text{d}_2$

The infrared and Raman spectra of dideuteroxyoxal are analogous in most respects to those of  $\text{C}_2\text{H}_2\text{O}_2$ . They clearly demonstrate the  $\text{C}_{2h}$  molecular symmetry of the trans molecules and  $\text{C}_i(\bar{1})$  site symmetry in the crystal since six fundamentals ( $2\text{A}_u + 4\text{B}_u$ ) appear strongly in the infrared spectrum and 6 ( $5\text{A}_g + \text{B}_g$ ) in the Raman spectrum. Admittedly there is a possible very slight breakdown of the rule of mutual exclusion due to the poly-crystalline environment of the molecules since a very weak infrared shoulder occurs at about  $1703\text{ cm}^{-1}$  ( $\nu_2(\text{A}_g) = 1709\text{ cm}^{-1}$ ) on the side of the



very intense  $\nu_{10}$  band, and an extremely weak Raman line at  $1681\text{ cm}^{-1}$  ( $\nu_{10}(B_u) = 1685\text{ cm}^{-1}$ ), but none of the other fundamentals are found in either spectrum in violation of the  $C_{2h}$  selection rules.

The observed frequencies are easily assigned to normal modes by comparison with the vapor data and an examination of the data reveals that, as for  $C_2H_2O_2$ , all vibration frequencies are higher in the solid than the vapor with the exception of the two carbonyl frequencies and, marginally,  $\nu_8$  the CD wagging mode. Some of the displacements from the vapor to the solid are quite large, e.g.  $+31$  and  $+47\text{ cm}^{-1}$  for the CH stretching modes,  $+32$  for the in-plane skeletal band,  $\nu_{12}$ ,  $+56\text{ cm}^{-1}$  for the torsion and  $-13$  and  $-29\text{ cm}^{-1}$  for the two carbonyl stretching modes. The shift in the torsion amounts to nearly 50% of the vapor frequency and an equally large change was noted for  $C_2H_2O_2$  [6,7]. This obviously is the result of very strong intermolecular interactions in the crystal. Dideutero-glyoxal does show some weak absorption at  $121\text{ cm}^{-1}$  (vapor torsion =  $118\text{ cm}^{-1}$ ), but we prefer to assign the very intense band at  $174\text{ cm}^{-1}$  to the torsion and that at  $121\text{ cm}^{-1}$  to a lattice mode.

As found for  $C_2H_2O_2$  only the C-D in-plane rocking band at  $1019, 1025\text{ cm}^{-1}$  exhibits factor group splitting, indicating that there must be at least two molecules per primitive unit cell. However, the absence of other such effects shows that vibrational coupling between molecules within the cell is not large.

The C-C stretching mode,  $\nu_4$ , appears clearly in the Raman spectrum at  $944\text{ cm}^{-1}$  (cf.  $1078\text{ cm}^{-1}$  for glyoxal). A number of weak bands in the infrared spectrum are assigned to binary combinations of one infrared-active mode and one Raman-active mode as indicated in Table I. No first overtones are allowed by the  $C_{2h}$  symmetry although  $2\nu_{10}$  appears weakly. The combination band  $\nu_3 + \nu_{11}(B_u)$

at  $2131\text{ cm}^{-1}$  is relatively intense and must be considered as a component of a Fermi doublet with  $\nu_9$  ( $B_u$ ) at  $2177\text{ cm}^{-1}$ . One overtone,  $2\nu_5$ , occurs in the Raman spectrum.

(b) Glyoxal- $d_1$

This compound gives a classical example of the breakdown of the principle of mutual exclusion on loss of the center of symmetry by partial deuteration. All twelve modes of  $C_2HDO_2$  ( $C_s$ ) can be both infrared- and Raman-active, but although the center of symmetry has gone the overall degree of asymmetry of the molecule is low, so that some transition probabilities will remain low. However, eight clear coincidences are observed. In the cases of  $C_2H_2O_2$  and  $C_2D_2O_2$ , the symmetrical carbonyl stretching vibration,  $\nu_2$ , is Raman-active and the antisymmetrical mode,  $\nu_{10}$ , is infrared-active. In  $C_2HDO_2$  both transitions occur in both types of spectrum, but  $\nu_2$  is very much the stronger in the Raman effect, and  $\nu_{10}$  very much the stronger in the infrared spectrum.

The clear coincidences occur at 2882, 2161, 1720, 1699, 1352, 1116, 1005 and  $981\text{ cm}^{-1}$  which are readily assigned to the CH stretch, CD stretch, symmetrical CO stretch, antisymmetrical CO stretch, CH rock, C-C stretch, C-H out-of plane wag and CD rock, respectively. In general, the agreement between the infrared and Raman frequencies is well within the accuracy of the instruments, but a small anomaly is noticed in the case of the symmetrical carbonyl stretch,  $\nu_2$ , where the infrared maximum occurs at  $1725\text{ cm}^{-1}$  and the Raman at  $1720\text{ cm}^{-1}$ . This discrepancy could be due to slight differences in the degree of crystallinity of the different solid samples, which were difficult to anneal because of high volatility.

The remaining fundamentals are easily identified at  $548\text{ cm}^{-1}$  (C-C=O symmetrical bend) in the Raman spectrum, and at  $710\text{ cm}^{-1}$  (CD out-of-plane wag),  $357\text{ cm}^{-1}$  (antisymmetric C-C=O bend) and  $193\text{ cm}^{-1}$  (torsion) in the infrared spectrum. It is interesting to note that three of these four fundamentals, for which the change of a hydrogen atom for a deuterium is insufficient to violate the  $C_{2h}$  selection rules, all involve principally motion only of the O=C-C=O skeleton.

Cole and Osborne [1] were unable to detect  $\nu_6$ , the C-D out-of plane wag<sup>†</sup> in the infrared spectra of  $C_2HDO_2$  and  $C_2D_2O_2$  vapor, although product rule calculations indicated that they would lie near  $638\text{ cm}^{-1}$  and  $630\text{ cm}^{-1}$  respectively. In the infrared spectra of the solids they are found at  $710\text{ cm}^{-1}$  and  $643\text{ cm}^{-1}$ .

The C-C stretching mode,  $\nu_4$ , is clearly indicated at about  $1116\text{ cm}^{-1}$  in both the Raman and infrared spectra. This frequency has been somewhat difficult to identify in the infrared spectrum of the vapor due to lack of resolvable rotational fine structure in the weak band found by Cole and Osborne [1]. It had been predicted to lie near  $1104\text{ cm}^{-1}$  on the basis of normal coordinate calculations by Fukuyama, Kuchitsu and Morino (see [1]) and was found at that frequency in the laser-excited emission spectrum of the vapor [8].

The infrared band due to  $\nu_{11}$  the in-plane CH rocking mode, is not subject to factor group splitting in contrast to the analogous bands of  $C_2H_2O_2$  and  $C_2D_2O_2$  mentioned above. This is an obvious consequence of the loss of symmetry in the monodeutero-compound.

---

<sup>†</sup>See footnote to Table 1.

A comparison of the frequencies of the solid and the vapor shows that monodeuteroglyoxal parallels the behaviour of glyoxal. Only the carbonyl stretching modes move to lower frequency on crystallization. Again, the torsional mode is drastically increased in frequency, this time to  $193\text{ cm}^{-1}$  (cf. vapor  $123\text{ cm}^{-1}$ ). Weak infrared absorption is found at 122, 133 and  $138\text{ cm}^{-1}$  but these are attributed to lattice modes.

First overtones and combinations are both allowed in the infrared spectrum of  $\text{C}_2\text{HDO}_2$  and a number have been assigned (Table II). In particular, it should be noted that all three combination modes,  $2\nu_2$ ,  $\nu_2+\nu_{10}$  and  $2\nu_{10}$ , involving the carbonyl stretching modes are observed.

Table III summarizes the vapor and solid data for the three trans-glyoxals.

Finally it should be noted that at the low sample temperatures used in the present work, no Raman lines or infrared bands attributable to cis-glyoxal [15-17] could be detected.

#### Acknowledgements

This work was carried out with the financial support of the National Aeronautics and Space Administration by grant NGL-41-002-003.

A travel grant to A.R.H.C. from the Australian-American Education Foundation, assistance with chemicals from Dr. J.D. Odom, and with equipment from Mr. M. Griffin and Miss D.B. Braund are also gratefully acknowledged.

## References

1. Cole, A.R.H. and Osborne, G.A.: Spectrochim. Acta 27A, 2461 (1971).
2. Paldus, J. and Ramsay, D.A.: Can. J. Phys. 45, 1389 (1967).
3. Birss, F.W., Brown, J.M., Cole, A.R.H., Lofthus, A., Krishnamachari, S.L.N.G., Osborne, G.A., Paldus, J., Ramsay, D.A., and Watmann, L.: Can. J. Phys. 48, 1230 (1970).
4. Agar, D.M., Bair, E.J., Birss, F.W., Borrell, P., Chen, P.C., Currie, G.N., McHugh, A.J., Orr, B.J., Ramsay, D.A., and Roncin, J.Y.: Can. J. Phys. 49, 323 (1971).
5. Holzer, W. and Ramsay, D.A.: Can. J. Phys. 48, 1759 (1970).
6. Verderame, F.D., Castellucci, E., and Califano, S.: J. Chem. Phys. 52, 719 (1970).
7. Durig, J.R. and Hannum, S.E.: J. Cryst. Mol. Struct. 1, 131 (1971).
8. Kho, Le Khyo and Tyulin, V.I.: Opt. Spektrosk. 35, 770 (1973).
9. Dong, R.Y. and Ramsay, D.A.: Can. J. Phys. 51, 1491 (1973).
10. Riley, H.L. and Friend, N.A.C.: J. Chem. Soc. 2342 (1932).
11. Durig, J.R. Riethmiller, S., and Li, Y.S.: J. Chem. Phys. 61, 253 (1974).
12. IUPAC "Tables of Wavenumbers for the Calibration of Infrared Spectrometers," Butterworths, London (1961).
13. Cole, A.R.H., Jones, R.N., and Lord, R.C.: Pure and Appl. Chemistry, 33, 605 (1973).
14. Baglin, F.G., Bush, S.F., and Durig, J.R.: J. Chem. Phys. 47, 2104 (1967).
15. Currie, G.W. and Ramsay, D.A.: Can. J. Phys., 49, 317 (1971).
16. Ramsay, D.A. and Zauli, C.: Acta Phys. Acad. Sci. Hung., 35, 79 (1974).
17. Durig, J.R., Tong, C.C., and Li, Y.S.: J. Chem. Phys., 57, 4425 (1972).

TABLE I. Infrared and Raman data on solid glyoxal-d<sub>2</sub>

Infrared $\nu(\text{cm}^{-1})$	Rel. Int.	Raman $\Delta\nu(\text{cm}^{-1})$	Rel Int.	Assignment
3887	w			$\nu_2 + \nu_9 = 3886$
3857	w			$\nu_1 + \nu_{10} = 3854$
3842	vw			
3383	w			$\nu_2 + \nu_{10} = 3394$
3361	w			$2\nu_{10} = 3370$
2339	vw			$\nu_1 + \nu_7 = 2343$
2236	w			$\nu_5 + \nu_{10} = 2228$
*2177	s			$\nu_9$
		2169	m	$\nu_1$
*2131	m			$\nu_3 + \nu_{11} = 2153$
2106	vw			
2052	vw			$\nu_2 + \nu_{12} = 2052$
1724	w			
1703	sh	1709	s	$\nu_2$
1694	w			
1685	vs	1681	w	$\nu_{10}$
1659	w			
1549	w			$\nu_6 + \nu_8 = 1551$
		1131	m	$\nu_3$
		1086	m	$2\nu_5$
1025 )				
)				
1019 )	vs			$\nu_{11}$
980				
		944	s	$\nu_4$
		908	m	$\nu_8^+$

(continued .....

TABLE I. (continued)

Infrared $\nu(\text{cm}^{-1})$	Rel. Int.	Raman $\Delta\nu(\text{cm}^{-1})$	Rel. Int.	Assignment
643	w			$\nu_6^{\dagger}$
		543	s	$\nu_5$
343	s			$\nu_{12}$
174	vs			$\nu_7$
121	w			Lattice mode

\* Fermi doublet

† Note that we have now followed Dong and Ramsay [9] in interchanging the numbering of  $\nu_6$  and  $\nu_8$  in comparison with that originally given by Cole and Osborne [1].

TABLE II. Infrared and Raman data on solid glyoxal-d<sub>1</sub>

Infrared $\nu(\text{cm}^{-1})$	Rel. Int.	Raman $\Delta\nu(\text{cm}^{-1})$	Rel. Int.	Assignment
3883	vw			$\nu_8 + \nu_9 = 3887$
3855	vw			( $\nu_3 + \nu_9 = 3863$ ( $\nu_1 + \nu_{10} = 3860$
3434	w			$2\nu_2 = 3440$
3401	m			$\nu_2 + \nu_{10} = 3419$
3373	w			$2\nu_{10} = 3398$
3073	w			$\nu_7 + \nu_9 = 3075$
2882	s	2882	m	$\nu_9$
2675	w			$\nu_3 + \nu_{10} = 2680$
2248	vw			$\nu_5 \nu_{10} = 2247$
2204	w			
2160	s	2161	m	$\nu_1$
2089	vw			$\nu_3 + \nu_4 = 2096$
2076	vw			$\nu_2 + \nu_{12} = 2077$
2064	w			$\nu_6 + \nu_{11} = 2062$
2005	w			$2\nu_8 = 2010$
1725	m	1720	s	$\nu_2$
1720	w			
1709	w			
1699	vs	1700	w	$\nu_{10}$
1694	w			$\nu_3 + \nu_6 = 1691$
1675	w			
1665	w			
1352	s	1352	m	$\nu_{11}$
1330	w			$\nu_3 + \nu_{12} = 1338$

(continued....)



TABLE II. (continued)

Infrared $\nu(\text{cm}^{-1})$	Rel. Int.	Raman $\Delta\nu(\text{cm}^{-1})$	Rel. Int.	Assignment
1116	m	1117	m	$\nu_4$
1092	m	1093	m	$2\nu_5 = 1096$
1021	w			
1005	m	1004	m	$\nu_8^\dagger$
980	s	982	m	$\nu_3$
710	w			$\nu_6^\dagger$
		560	w	$\nu_7 + \nu_{12} = 550$
553	vw	548	s	$\nu_5$
357	vs			$\nu_{12}$
193	vs			$\nu_7$
138	w			Lattice mode
133	w			Lattice mode
122	w			Lattice mode

<sup>†</sup> See footnote to Table I.

TABLE III. Comparison of fundamental frequencies of the glyoxals in solid and gas phases

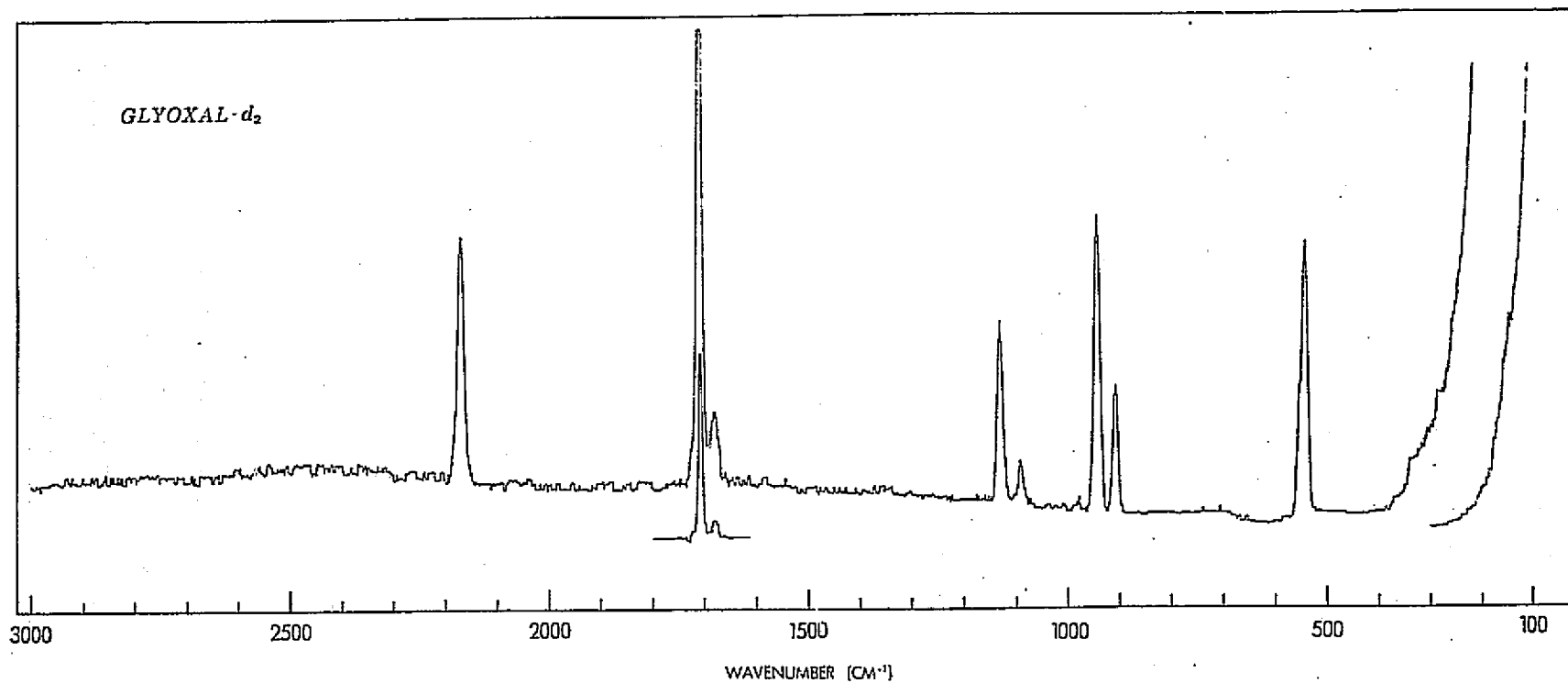
		$\text{C}_2\text{H}_2\text{O}_2$		$\text{C}_2\text{D}_2\text{O}_2$		$\text{C}_2\text{HDO}_2$	
		Solid [7]	Gas [1,9]	Solid	Gas [1,9]	Solid	Gas [1,9]
$A_g$							
$\nu_1$	C-H(D) stretching	2882	2843	2169	2138	2161	2130.2
$\nu_2$	C=O stretching	1729	1745	1709	1722	1720	1735
$\nu_3$	C-H(D) rocking	1364	1338	1131	1130	981	971.6
$\nu_4$	C-C stretching	1078	1065	944	932	1116	1104
$\nu_5$	C-C=O bending	551	550.53	543	537.29	548	542
$A_u$							
$\nu_6$	C-H(D) wagging	842	801.4	643	630	710	688
$\nu_7$	torsion	192	126.7	174	117.98	193	122.8
$B_g$							
$\nu_8$	C-H wagging	1050	1047.91	908	909	1005	999
$B_u$							
$\nu_9$	C-H(D) stretching	2890	2835.07	2177	2130	2882	2835.2
$\nu_{10}$	C=O stretching	1707	1732	1685	1710	1699	1717
$\nu_{11}$	C-H(D) rocking	1333, 1326	1312.4	1025, 1019	1010.1	1352	1335
$\nu_{12}$	C-C=O bending	388	338.6	343	311.1	357	323.7

Captions for figures

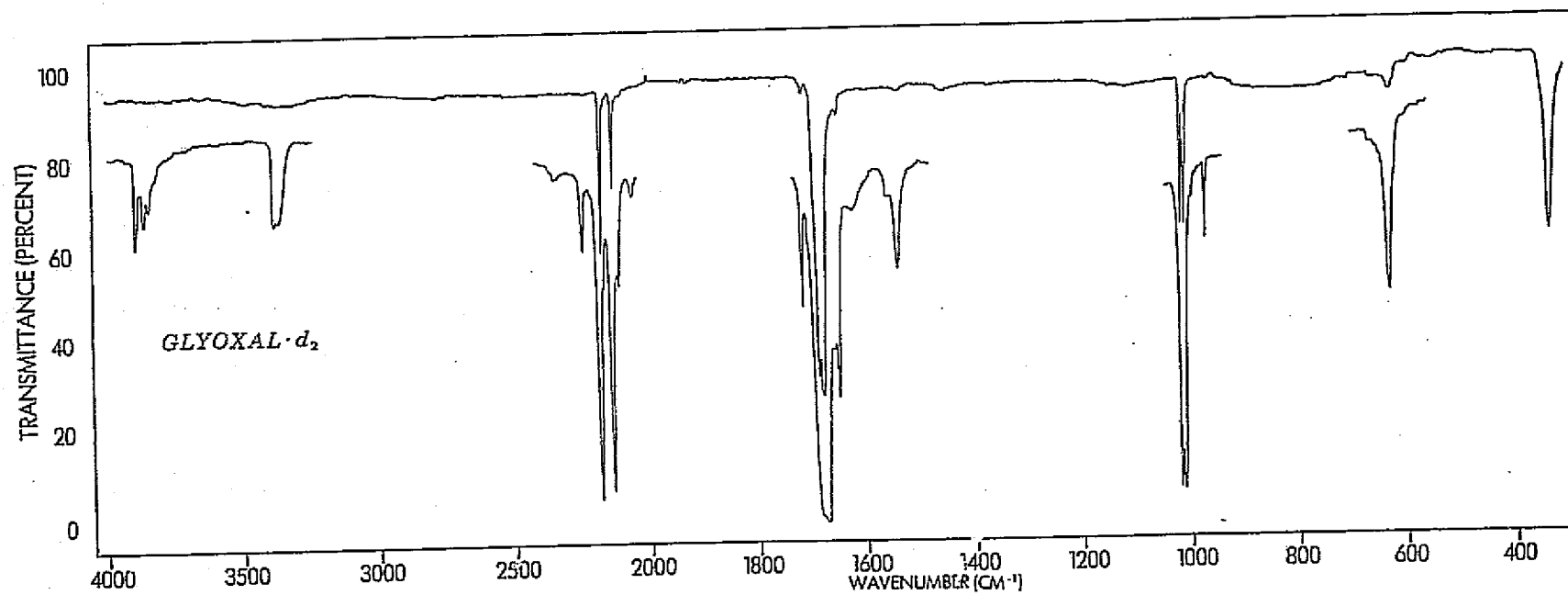
(Cole and Durig)

- Figure 1. The Raman spectrum of solid glyoxal-d<sub>2</sub>
- Figure 2. The mid-infrared spectrum of solid glyoxal-d<sub>2</sub>
- Figure 3. The far-infrared spectrum of solid glyoxal-d<sub>2</sub>
- Figure 4. The Raman spectrum of solid glyoxal-d<sub>1</sub>. Small gaps indicate the positions of unfiltered plasma lines from the laser.
- Figure 5. The mid-infrared spectrum of solid glyoxal-d<sub>1</sub>
- Figure 6. The far-infrared spectrum of solid glyoxal-d<sub>1</sub>

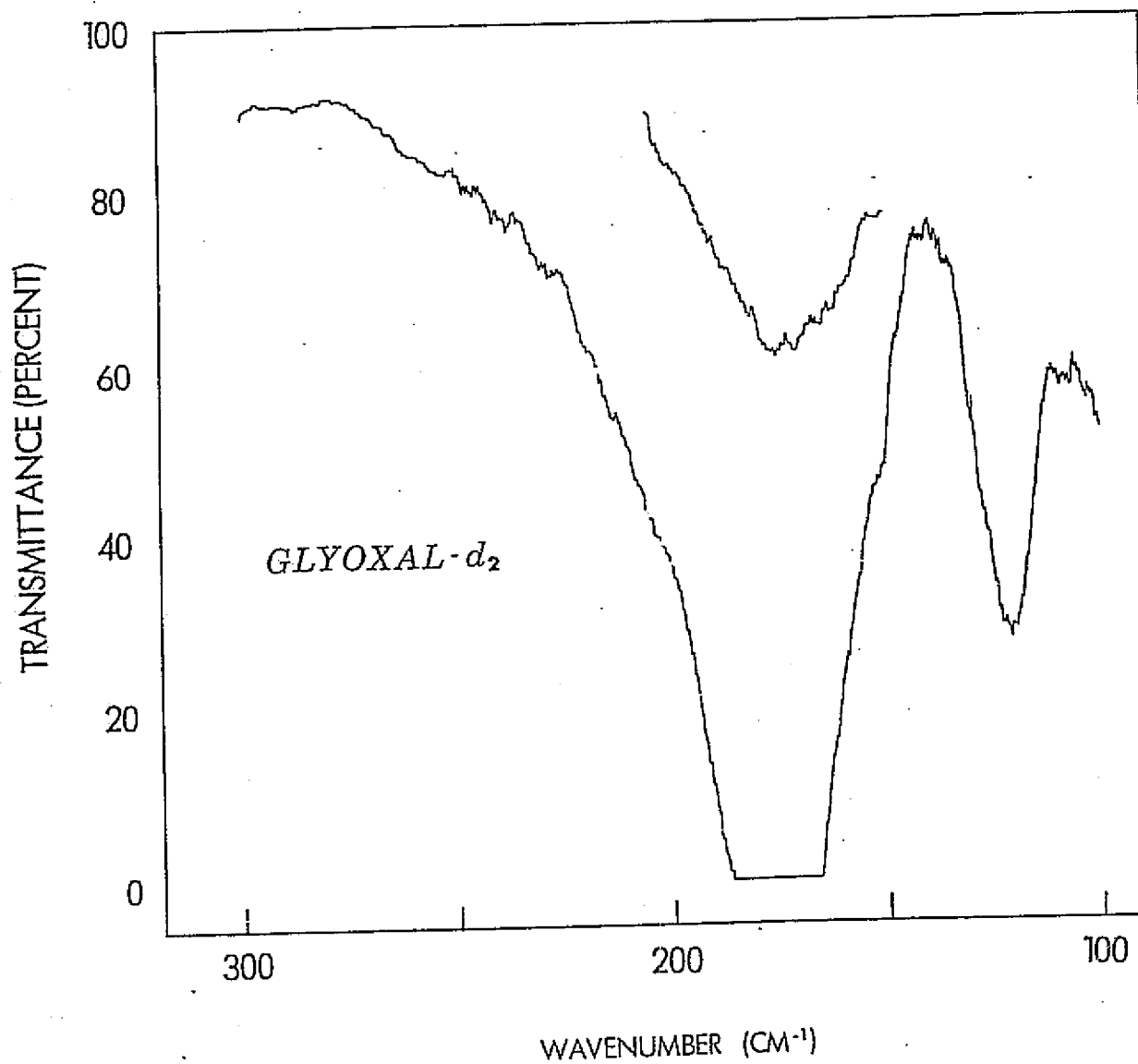
Lab and Data Fig 1



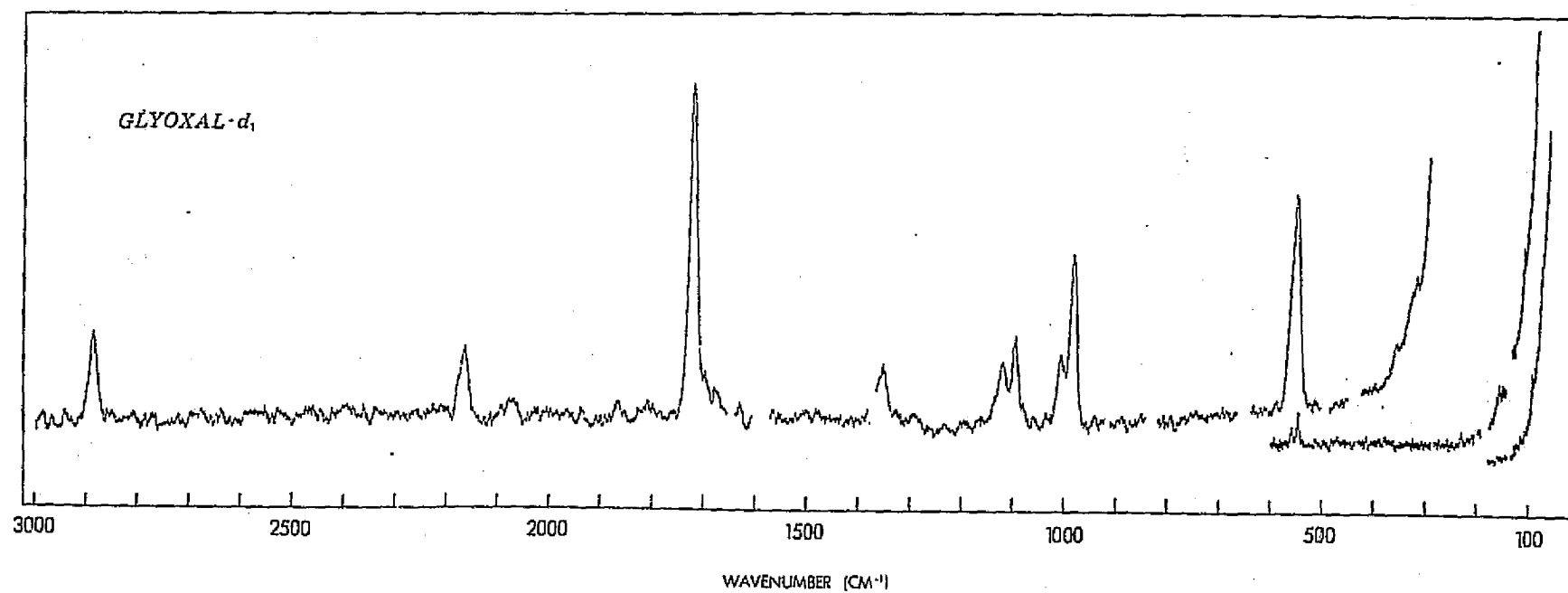
ORIGINAL PAGE IS  
OF POOR QUALITY



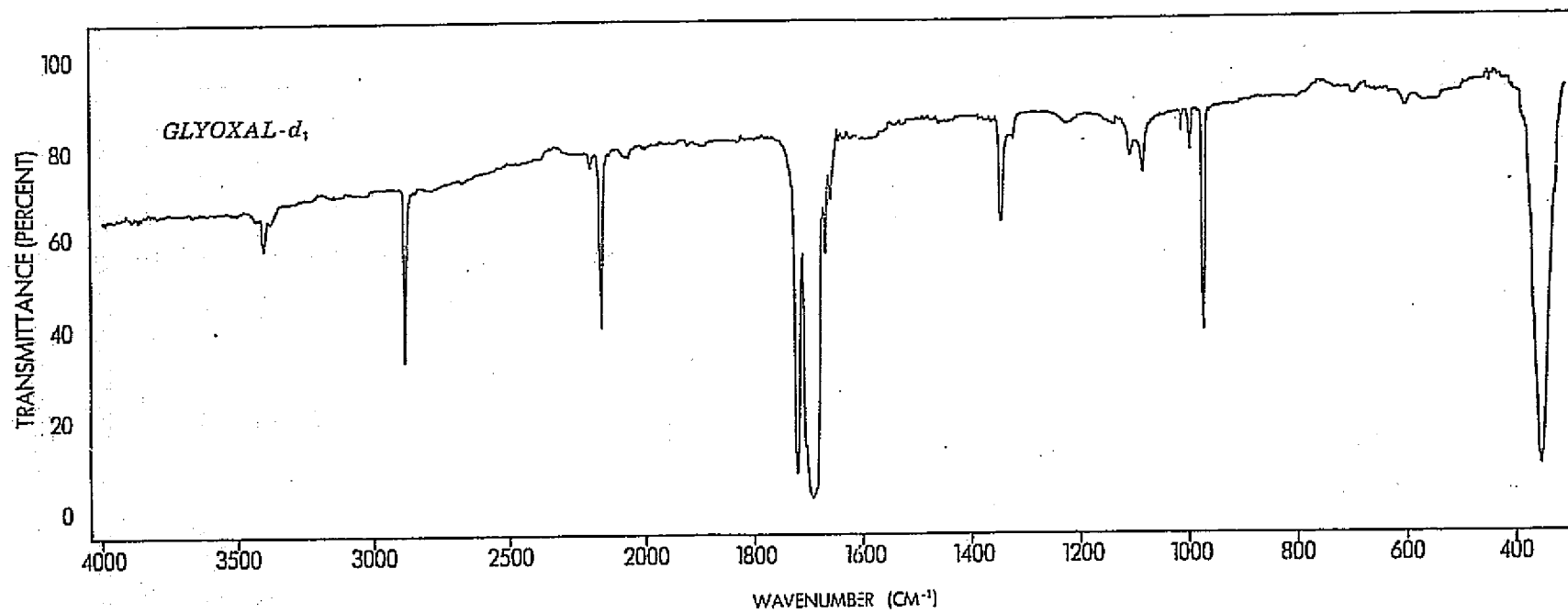
ORIGINAL PAGE IS  
OF POOR QUALITY



Cell and Drying Fig 4

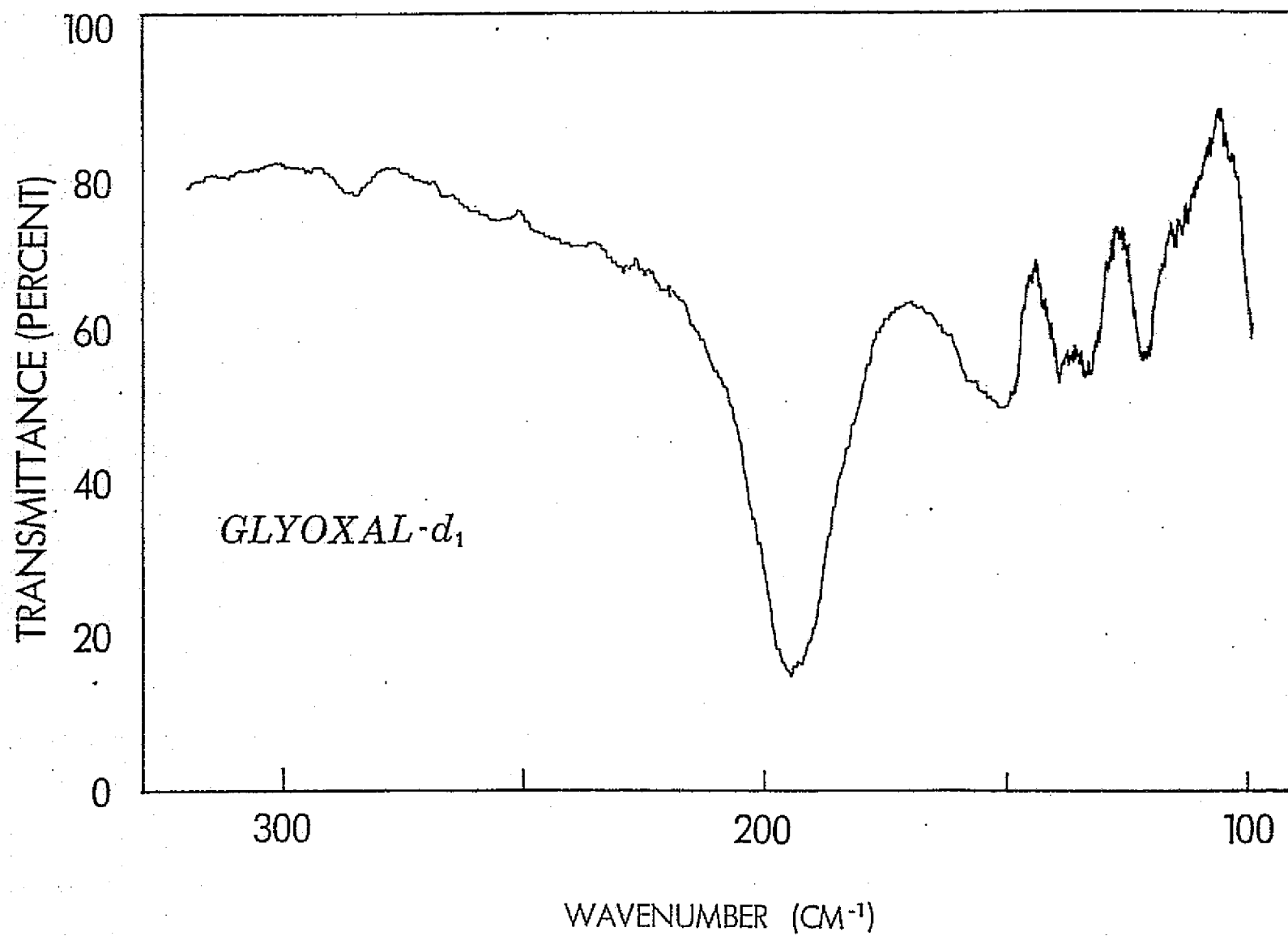


Cole and Dreyer May 5





ORIGINAL PAGE IS  
OF POOR QUALITY



## APPENDIX II

### MICROWAVE AND RAMAN SPECTRA, DIPOLE MOMENT, BARRIER TO INTERNAL ROTATION, AND VIBRATIONAL ASSIGNMENT OF SILYLPHOSPHINE-d<sub>2</sub>

ABSTRACT. The microwave spectrum of  $\text{SiH}_3\text{PD}_2$  have been recorded in the range 26.5 to 40.0 GHz. Both a- and c- type transitions were observed and assigned. The rigid rotor rotational constants were determined to be:  $A = 37589.06 \pm 0.11$ ,  $B = 5315.70 \pm 0.02$  and  $C = 5258.70 \pm 0.02$  MHz. The barrier to internal rotational has been calculated from the A - E splittings to be  $1512 \pm 26$  cal/mole. The dipole moment components of  $|\mu_a| = 0.22 \pm 0.01$ ,  $|\mu_c| = 0.56 \pm 0.01$ , and  $|\mu_t| = 0.60 \pm 0.01$  D were determined from the Stark effect. By using previously determined microwave data for  $\text{SiH}_3\text{PH}_2$ , several structural parameters have been calculated and their values are compared to similar ones in other compounds. The Raman (0 - 2500  $\text{cm}^{-1}$ ) spectra of gaseous, liquid and solid  $\text{SiH}_3\text{PH}_2$  and gaseous  $\text{SiH}_3\text{PD}_2$  have been recorded and interpreted in detail on the basis of  $C_s$  molecular symmetry.

---

## INTRODUCTION

We have been interested<sup>1</sup> for some time in the magnitude of the barriers to internal rotation around single bonds. Much of the reliable data now available on barrier heights is for C - C or C - X (where X = Si, Ge, N, P, O, S) bonds and there is little information available on the barriers to internal rotation around Si - X (where X = N, P, O, S) bonds. As part of a broad program to evaluate such barriers we recorded<sup>2</sup> the microwave spectrum of silylphosphine but during the course of our work a preliminary study of the microwave spectrum of this molecule was reported.<sup>3</sup> However there have been no reported microwave or vibrational studies of silylphosphine-d<sub>2</sub>.

Linton and Nixon<sup>4</sup> reported the infrared (300 - 4000 cm<sup>-1</sup>) spectrum in the gas phase of silylphosphine and suggested that the overtone of the torsion was in the 480 cm<sup>-1</sup> range. Additionally these authors<sup>4</sup> assigned six of the remaining fourteen fundamentals positively and a further seven tentatively but point out that the spectra of several deuterated species would be quite valuable in assessing the correctness of their assignments. More recently Drake and Riddle<sup>5</sup> reported the infrared spectrum of gaseous SiD<sub>3</sub>PD<sub>2</sub> and carried out a normal coordinate calculation for both the "light" and totally deuterated species. On the bases of these studies, these authors<sup>5</sup> reassigned the deformational motions for the "light" compound. However they<sup>5</sup> stress that the exact geometry of the silylphosphine is unknown so that their results could be subject to considerable error on this point alone. Additionally their data was limited to above 400 cm<sup>-1</sup> so that

no information was obtained on the internal torsional mode. There have been no published Raman data on any of the isotopic species of silylphosphine. Thus, we have recorded the Raman spectra of silylphosphine in the gaseous, liquid and solid states and the Raman spectrum of silylphosphine- $d_2$  in the gaseous state to provide additional data for making vibrational assignments for the normal modes.

### EXPERIMENTAL SECTION

With the exception of the phosphine syntheses, all preparative work was carried out in a conventional high-vacuum system employing greaseless stopcocks.<sup>6</sup> Aluminum phosphide and silicon tetrachloride were obtained commercially (Alfa Inorganics) and used without further purification. Phosphine was prepared under a stream of nitrogen in a fume hood as described in the literature.<sup>7</sup> Phosphine- $d_3$  was prepared in a similar manner using  $D_2O$  and  $D_2SO_4$ . All phosphine species were purified by passing them through a  $-131^\circ$  bath ( $n-C_5H_{12}$  slush) into a  $-196^\circ$  bath. Purity was monitored by vapor pressure measurements<sup>8</sup> and infrared spectra<sup>9</sup>.

Silane was prepared as described in the literature.<sup>10</sup> Silylphosphine and silylphosphine- $d_2$  were prepared by heating a 1:1 mixture of  $SiH_4$  and  $Ph_3$  (or  $PD_3$ ) along with a trace of iodine to  $300^\circ C$ .<sup>11</sup> Final purification of silylphosphine species was achieved by use of a low temperature vacuum fractionation column<sup>12</sup>. Purity was monitored by vapor pressure measurement<sup>13</sup> and infrared spectra<sup>4, 5</sup>.

The microwave spectrum was obtained using a Hewlett Packard Model 8460 A MRR microwave spectrometer with a Stark modulation frequency of 33.33 kHz. All the frequency measurements were taken with the Stark cell cooled with dry ice and no appreciable decomposition of the sample in the waveguide was noticed. The accuracy of the measured frequency was estimated to be better than 0.1 MHz.

The Raman spectra were recorded on a Cary Model 82 Raman spectrophotometer equipped with an argon-ion laser with a frequency of  $5145 \text{ \AA}$  for excitation. The Raman spectrum of the solid was obtained using a cold cell similar to the one described earlier for far infrared<sup>14</sup> studies, except that the sample holder consists of a blackened brass block at an angle of  $75^\circ$  from the normal. The Raman spectrum of the liquid was obtained by sealing the sample in a glass capillary. The Raman spectrum of the gas was obtained at room temperature in a standard Cary multipass cell and the laser was multipassed through the cell. The spectra of  $\text{SiH}_3\text{PH}_2$  in solid, liquid and gas phases are shown in Figure 1A, B, and C and the spectrum of  $\text{SiH}_3\text{PD}_2$  in the gas phase is shown in Figure 1D and the observed frequencies are listed in Tables I and II.

#### VIBRATIONAL ASSIGNMENT

Since silylphosphine has  $C_s$  point group symmetry, the 15 fundamental vibrations belong to the following irreducible representations:  $9A' + 6A''$ . For these fundamental motions, nine modes will result from primarily Si-H motions ( $5A' + 4A''$ ) and five modes from the P-H motions ( $3A' + 2A''$ ). Both the  $A'$  and  $A''$  species are Raman active with the fundamentals belonging to the  $A'$  species

giving rise to polarized Raman lines whereas those belonging to the A" species should give rise to depolarized lines. Thus, the depolarization data should make it possible to confirm or reject some of the earlier assignments for the normal modes.

### SiH<sub>3</sub> Modes

There are three Si-H stretching motions but there are only two bands observed in the expected frequency region in the Raman spectra of the gaseous, liquid and solid SiH<sub>3</sub>PH<sub>2</sub>. The polarized bands at 2178 and 2152 cm<sup>-1</sup> in the Raman spectrum of liquid H<sub>3</sub>SiPH<sub>2</sub> (2189 and 2166 in the gas phase) are assigned to  $\nu_2$  and  $\nu_3$ , respectively. The A" antisymmetric stretching mode,  $\nu_{11}$ , is expected to give rise to a weak Raman band and is probably hidden by the rather intense band at 2178 cm<sup>-1</sup>. The deuteration of the PH<sub>2</sub> group shifts the corresponding  $\nu_2$  and  $\nu_3$  bands in H<sub>3</sub>SiPD<sub>2</sub> to 2198 and 2186 cm<sup>-1</sup>, respectively. The differences in the Si-H stretching frequencies between the -d<sub>0</sub> and -d<sub>2</sub> species is caused by the coupling between the P-H and the Si-H stretching motions which occurs in the SiH<sub>3</sub>PH<sub>2</sub> molecule but not in SiH<sub>3</sub>PD<sub>2</sub>.

The antisymmetric SiH<sub>3</sub> deformations,  $\nu_5$  and  $\nu_{12}$ , are assigned to the band at 955 cm<sup>-1</sup> in the Raman spectrum of liquid H<sub>3</sub>SiPH<sub>2</sub>. The corresponding modes are observed near 940 cm<sup>-1</sup> in the spectrum of gaseous SiH<sub>3</sub>PD<sub>2</sub>. The same vibrations are also observed near 940 cm<sup>-1</sup> in the spectrum of the polycrystalline material. The symmetric silyl deformation,  $\nu_6$ , is assigned to the polarized band at 930 cm<sup>-1</sup> in the Raman spectrum of liquid SiH<sub>3</sub>PH<sub>2</sub>. This band is more intense than the corresponding antisymmetric deformational band in the liquid and solid and the  $\nu_5$  band appears as a shoulder on  $\nu_6$ . In the spectrum of gaseous SiH<sub>3</sub>PD<sub>2</sub>, broad bands near 940 and 927 cm<sup>-1</sup> are observed and are assigned to the antisymmetric and the symmetric deformations, respectively.

In  $\text{SiH}_3\text{PH}_2$ , the  $A'$  and  $A''$  silyl rocking modes,  $\nu_8$  and  $\nu_{14}$ , are observed at 600, 597 and 602  $\text{cm}^{-1}$  in the liquid, solid and gas, respectively. The same modes ( $\nu_8$  and  $\nu_{14}$ ) for  $\text{SiH}_3\text{PD}_2$  are assigned to the single line at 605  $\text{cm}^{-1}$ .

There was no observed band which could be assigned to the torsional motion of silyl group in either  $\text{SiH}_3\text{PH}_2$  or  $\text{SiH}_3\text{PD}_2$  molecule. However with the three-fold barrier (see Table V) and the molecular structure obtained from the microwave study, the torsional transition is calculated to have frequencies of 168 and 143  $\text{cm}^{-1}$  for  $\text{SiH}_3\text{PH}_2$  and  $\text{SiH}_3\text{PD}_2$ , respectively.

### PH<sub>2</sub> Modes

In silylphosphine- $d_0$ , the P-H stretch is expected to have the highest frequency and the polarized band at 2293  $\text{cm}^{-1}$  in the Raman spectrum of the liquid can be easily assigned to the  $A'$   $\text{PH}_2$  symmetric stretch,  $\nu_1$ . The same motion is observed at 2287 and 2304  $\text{cm}^{-1}$  for the solid and the gas, respectively. In the Raman spectrum of the gas a band appears as a shoulder at 2318  $\text{cm}^{-1}$  on the high frequency side of the symmetric  $\text{PH}_2$  stretching band and is assigned to the  $A''$   $\text{PH}_2$  stretch. In the Raman spectra of the liquid and solid, this motion was not observable due to overlapping by the symmetric  $\text{PH}_2$  stretch. In the Raman spectrum of gaseous  $\text{SiH}_3\text{PD}_2$  the antisymmetric and symmetric  $\text{PD}_2$  stretches were observed at 1597 and 1587  $\text{cm}^{-1}$ , respectively.

The  $\text{PH}_2$  scissor,  $\nu_4$ , is observed at 1100  $\text{cm}^{-1}$  as a very weak polarized line in the Raman spectrum of liquid  $\text{SiH}_3\text{PH}_2$ . No corresponding lines are observed in the spectra of the solid and gaseous materials. This mode was observed in the spectrum of  $\text{SiH}_3\text{PD}_2$  at 810  $\text{cm}^{-1}$  as a very weak line.

A depolarized band at 770  $\text{cm}^{-1}$  is assigned to the  $\text{PH}_2$  twisting mode,  $\nu_{13}$  for the "light" compound. This motion is mixed with the  $A''$   $\text{SiH}_3$  rocking mode in both  $\text{SiH}_3\text{PH}_2$  and  $\text{SiH}_3\text{PD}_2$ . A corresponding line at 763  $\text{cm}^{-1}$  is observed in the spectrum of the polycrystalline solid  $\text{SiH}_3\text{PH}_2$ . Deuteration of the  $\text{PH}_2$  group shifts this band to 657  $\text{cm}^{-1}$ .

For silylphosphine- $d_0$ , the  $PH_2$  wagging motion is expected to have the lowest frequency of all the  $PH_2$  modes. This vibration is observed at  $725\text{ cm}^{-1}$  as a very weak line in the Raman spectrum of the liquid. Corresponding lines are also observed in the spectra of the gas and solid. According to the normal coordinate analysis, this motion is mixed with the  $SiH_3$  rock. With deuteration of the  $PH_2$  group, the wagging motion is not only mixed with the  $SiH_3$  rock but also with the P-Si stretch. The line at  $552\text{ cm}^{-1}$  is, thus, assigned to the  $PD_2$  wag.

### Si-P Mode

The Si-P stretching vibration can be assigned unambiguously to the bands at  $452$ ,  $445$  and  $455\text{ cm}^{-1}$  in the solid, liquid and gaseous phase Raman spectra of  $SiH_3PH_2$ . With deuteration of the  $PH_2$  group, this mode shifts to  $427\text{ cm}^{-1}$ . Polarization measurements in the liquid state of  $SiH_3PH_2$  and the gaseous state of  $SiH_3PH_2$  and the gaseous state of  $SiH_3PD_2$  show that the bands are polarized as expected for the Si-P motion.

### Teller-Redlich Product Rule Calculations.

An attempt to check the consistency of the isotopic assignments was made through the Teller-Redlich product rule. Generally, an agreement of 3-4% is sufficient to suggest the general validity of the vibrational assignments. In the  $A'$  and  $A''$  ratios of  $d_2/d_0$ , the theoretical  $\tau$  values obtained by using the microwave experimental moments of inertia are 2.67 and 2.32, respectively. The vibrational assignments listed in Tables I and II give observed  $\tau$  values of 2.59 and 2.22 for the  $A'$  and  $A''$  ratios, respectively; both of these values are well within the uncertainties expected for these quantities. Initially, it was thought that the  $PD_2$  twist,  $\nu_{13}$ , was at  $498\text{ cm}^{-1}$  because of the normal coordinate calculation but such a value gave a totally unrealistic  $\tau$  value for the  $A''$  symmetry block.

We have also carried out Teller-Redlich product rule calculations for the totally deuterated molecule and the assignments proposed by Drake and Riddle. The



theoretical  $\tau$  values calculated from the microwave structure are 13.65 and 7.15 for the A' and A'' species, respectively. The proposed assignments of Drake and Riddle gave  $\tau$  values of 13.18 and 8.38 for these symmetry species, respectively. The agreement for the A' block is satisfactory but the value of 8.38 is in error in the wrong direction. It should be mentioned that this A'' symmetry block includes a calculated value for the  $\text{PH}_2$  twist which is probably too low. Additionally, the interchange of the assignments for the  $\text{SiD}_3$  symmetric and anti-symmetric deformations would improve the agreement between the observed and calculated  $\tau$  values.

#### NORMAL COORDINATE ANALYSIS

Although Drake and Riddle<sup>5</sup> have reported a normal coordinate calculation for  $\text{SiH}_3\text{PH}_2$  and  $\text{SiD}_3\text{PD}_2$ , they stressed the unknown structural parameters of the molecule with which the G matrix of the molecular motions were calculated. Since we have proposed a molecular structure from the results of the microwave investigation and since we have reassigned some of the vibrational modes for  $\text{SiH}_3\text{PH}_2$  in addition to assigning the vibrational spectrum of a new species,  $\text{SiH}_3\text{PD}_2$ , a normal coordinate calculation was carried out to obtain a valence force field (VFF) for silylphosphine. A basis set of 16 internal coordinates corresponding to those used by Wu, et al.<sup>15</sup> for the molecule methylamine was adopted to specify the symmetry coordinates. Twelve force constants have been chosen, which included eight principal and four interaction force constants. Schachtschneider's programs<sup>16</sup> were used to obtain a least-squares fit to the assigned frequencies and they were reproduced to within an average of  $8\text{ cm}^{-1}$  (see Tables I, II & III) with the force constants listed in Table IV. The diagonal force constants are essentially the same as those previously reported with the exception of the Si-P-H bending force constant which is 10% lower than the value reported earlier.<sup>5</sup> Also, we found the most significant interaction constant to be the SiH stretch/PSiH bend which had a value of  $0.14 \pm 0.10\text{ mdyne/\AA}$ . Other interaction constants were relatively small.

## MICROWAVE SPECTRUM

Silylphosphine has a symmetry plane which contains the a and c principal axes; consequently only a- and c- type transitions are expected. The molecule is very nearly a prolate rotor and the c-type Q-branch series,  $J_{1,J} \leftarrow J_{0,J}$ , transitions were easily recognized from their regular spacing and Stark splittings. All the Q-branch transitions were observed to have a splitting of about 20 MHz which is caused by the tunnel effect of the torsional motion of the silyl group. With the Q-branch assignment, a reasonably good value of  $A - C$  and  $\kappa$  were obtained. A- type transitional frequencies were initially predicted from the combined information on  $A - C$ ,  $\kappa$  and the rotational constant  $C$  which was calculated from the electron diffraction structure<sup>17</sup>. This prediction gave a very good estimate where one should expect the  $3 \leftarrow 2$  transitions. Further identification of the lines was made from their Stark effect and the splitting due to the internal rotation. Since the molecule is very nearly a symmetric rotor, the  $\kappa = 0$  and 2 lines of the  $J = 3 \leftarrow 2$  transition are too close in frequency to be resolved. The A - E splittings of these two transitions were predicted to be less than 0.2 MHz. For these reasons, only a single line was observed for all three of these transitions. Listed in Table V are the A state transitional frequencies of  $\text{SiH}_3\text{PD}_2$  in the ground vibrational state along with the difference calculated from the rigid rotor model. The effective rotational constants listed in Table VI were obtained from these frequencies.

## STRUCTURE

The present microwave study has provided limited information for obtaining a good molecular structure for silylphosphine. However, a well determined Si-P bond distance has been reported by Glidewell, et al.<sup>17</sup> from their electron diffraction investigation of  $\text{SiH}_3\text{PH}_2$ . This bond length is believed to be the most sensitive parameter in determining the observed rotational constants B and C. For this reason, we fixed the Si-P bond distance ( $2.249 \text{ \AA}$ ) and assumed a Si-H bond length ( $1.490 \text{ \AA}$ ) in order to obtain a set of structural parameters which gave the best reproducible rotational constants for both  $\text{SiH}_3\text{PH}_2$  ( $A = 51861.7$ ;  $B = 5581.48$ ;  $C = 5556.50 \text{ MHz}$  which were obtained for the A lines of the A-E internal rotation doublets<sup>3</sup>) and  $\text{SiH}_3\text{PD}_2$  species. (In calculating the proposed structure, the same P-H and P-D distances were assumed). The parameters obtained are:  $r(\text{P-H}) = 1.420 \text{ \AA}$ ,  $\angle \text{PSiH} = 111.4^\circ$ ,  $\angle \text{HPH} = 93.9^\circ$ , and  $\angle \text{SiPH} = 92.8^\circ$ . With these parameters, we calculated all the rotational constants within 3 MHz of the experimental values.

It is difficult to determine the accuracy of these parameters. If a tilt angle of 2 degrees is assumed for the silyl group toward the lone-pair electrons of the  $\text{PH}_2$  group, the resultant parameters obtained by the same procedures did not show any significant difference from the previous values. If a Si-H distance of  $1.50 \text{ \AA}$  is assumed, the P-H distance is only  $0.003 \text{ \AA}$  shorter and the HPH angle was only  $0.2^\circ$  larger than the corresponding values obtained in the first calculation, while the PSiH and SiPH angles were  $0.9$  degree larger and  $1.3$  degree smaller than the previous determined values, respectively.

## DIPOLE MOMENT

The dipole moment of  $\text{SiH}_3\text{PD}_2$  was determined by measuring the quadratic Stark effects of the following components:  $|M| = 3$  of the  $3_{13} \leftarrow 3_{03}$ ,  $|M| = 4$  of the  $4_{14} \leftarrow 4_{04}$  and  $|M| = 4$  and  $5$  of the  $5_{15} \leftarrow 5_{05}$  transitions. The electric field was calibrated from the measured Stark effect of the  $J = 3 \leftarrow 2$  transition of the OCS molecule and its dipole moment<sup>18</sup> of  $0.71521\text{D}$ . The analysis was carried out by the method of Golden and Wilson<sup>19</sup> and the out of the symmetry plane component,  $\mu_b$ , was assumed to be zero. The dipole moment components of  $|\mu_a|$  and  $|\mu_c|$  were found to be  $0.22 \pm 0.01$  and  $0.56 \pm 0.01\text{D}$ , respectively, and the total dipole moment,  $|\mu_t|$ , was found to have a value of  $0.60 \pm 0.01\text{D}$ . These results are listed in Table VII.

## INTERNAL ROTATION

Most of the observed ground state transitions for  $\text{SiH}_3\text{PD}_2$  have resolvable A and E state lines due to the internal rotation of the silyl group along the SiP bond. These splittings are listed in Table VIII. The same method as adopted previously<sup>20</sup> was used to determine the barrier to internal rotation. The internal rotational parameters  $F = 152.4 \text{ kHz}$ ,  $\alpha = 0.4408$  and  $\gamma = 0.0011$  (see Table VIII) as required in the barrier calculations were derived from the molecular structure obtained in the electron diffraction study<sup>17</sup> with an assumption of a "tilt" angle of 2 degrees. With these parameters and from each splitting one obtains a barrier to internal rotation as listed in Table VIII under column  $V_3$ . These values are found to be consistent with each other and the average value,  $\bar{V}_3$ , is  $1512 \text{ cal/mole}$  with a standard deviation of  $6 \text{ cal/mole}$ . A

possible error of 0.2 MHz in the measured splitting will cause a maximum deviation of 20 cal/mole for the barrier. If considerations are given only to the consistency of the barrier obtained from the different transitions and the possible experimental error of the frequency measurement, the resultant barrier to internal rotation is  $V_3 = 1512 \pm 26$  cal/mole.

## DISCUSSION

In an electron diffraction study of  $\text{SiH}_3\text{PH}_2$ , Glidewell, et al.<sup>17</sup> have concluded that there is little contribution of the 3d orbitals of silicon to the Si-P bond. They also concluded that the substitution of the  $\text{SiH}_3$  for  $\text{CH}_3$  in  $\text{CH}_3\text{PH}_2$  did not change appreciably the structure of the  $\text{PH}_2$  moiety. Although the accuracy of our present structural determination prevents us from making any quantitative comparison strictly with other similar molecules, it would be of interest to qualitatively compare structural parameters. For instance, the HPH angle of  $93.9^\circ$  is close to the corresponding angle of  $93.3^\circ$  found in phosphine<sup>21</sup>. A similar value of the SiPH angle ( $92.8^\circ$ ) is also found in silylphosphine. The value of  $r(\text{P-H})$  of  $1.42 \text{ \AA}$  is comparable to the corresponding bond distance of  $1.420 \text{ \AA}$  found in phosphine.<sup>21</sup> From this comparison, it appears that the chemical bonding involving the phosphorus atom after the substitution of a silyl group for H in phosphine does not change drastically.

The barrier to internal rotation (1.51 kcal/mole) obtained in the present study for silylphosphine is apparently smaller than that of methylphosphine (1.96 kcal/mole)<sup>22</sup>. The absence of d-orbital participation in the chemical bonding has made it possible to compare the contributions of the nonbonded interactions to the barriers in these two molecules. Because of the smaller barrier in silylphosphine than in methylphosphine, it is concluded that silylphosphine has significantly smaller contributions to the internal rotational barrier from the nonbonded inter-

actions than methylphosphine. These smaller interactions probably arise from the fact that the Si-P distance ( $2.249 \text{ \AA}$ ) is longer in silylphosphine than the C-P distance ( $1.863 \text{ \AA}$ ) in methylphosphine.

#### ACKNOWLEDGMENT

The authors gratefully acknowledge the financial support of this work by the National Aeronautics and Space Administration by grant NGL-41-002-003.

## REFERENCES

1. J. R. Durig, S. M. Craven and W. C. Harris, in Vibrational Spectra and Structure (J. R. Durig, ed.), Volume 1, Marcel Dekker Inc., New York (1972), p. 73.
2. M. M. Chen, M. S. Thesis, University of South Carolina, Columbia, South Carolina (1972).
3. R. Varma and K. R. Ramaprasad, 4th Austin Symposium on Gas Phase Molecular Structure, Austin, Texas, 1972. Paper T5; K. R. Ramaprasad, Ph. D. Thesis, New York Univ., 1972.
4. H. R. Linton and E. R. Nixon, *Spectrochim. Acta*, 11, 146 (1959)
5. J. E. Drake and C. Riddle, *Spectrochim. Acta*, 26A, 1697 (1970).
6. D. F. Shriver, "The Manipulation of Air-Sensitive Compounds," McGraw-Hill, New York, N. Y., 1969.
7. R. C. Marriott, J. D. Odom and C. T. Sears, *Inorg. Syn.* 14, 1 (1973).
8. S. R. Gunn and L. G. Green, *J. Phys. Chem.* 65, 779 (1961).
9. D. A. Tierney, D. W. Lewis and D. Berg, *J. Inorg. Nucl. Chem.* 24, 1165 (1962).
10. A. D. Norman, J. R. Webster and W. L. Jolly, *Inorg. Syn.* 11, 170 (1968).
11. I. H. Sabherwal and A. B. Burg, *Inorg. Nucl. Chem. Letters* 8, 27 (1972).
12. J. Dobson and R. Schaeffer, *Inorg. Chem.* 9, 2183 (1970).
13. C. Glidewell and G. M. Sheldrick, *J. Chem. Soc. (A)*, 350 (1969).
14. F. G. Baglin, S. F. Bush and J. R. Durig, *J. Chem. Phys.* 47, 2104 (1967).
15. E. L. Wu, G. Zerbi, S. Califano, and B. Crawford, Jr., *J. Chem. Phys.*, 35 2060 (1961).
16. J. H. Schachtschneider, "Vibrational Analysis of Polyatomic Molecules, V and VI", Technical Report Nos. 231-64 and 57-65, Shell Development Company.

17. C. Glidewell, P. M. Pinder, A. G. Robiette, and G. M. Sheldrick, J. Chem. Soc., Dalton 1402 (1973).
18. J. S. Muentner, J. Chem Phys. 48, 4544 (1968).
19. S. Golden and E. B. Wilson, Jr., J. Chem. Phys. 16, 669 (1948).
20. J. R. Durig, K. L. Kizer and Y. S. Li, J. Amer. Chem. Soc., 96, 7400 (1974).
21. C. A. Burrus, J. Chem. Phys., 28, 428 (1958).
22. T. Kojima, E. L. Breig, and C. C. Lin, J. Chem. Phys., 35, 2139 (1961).



Table I. Observed and Calculated Raman frequencies ( $\text{cm}^{-1}$ ) of  $\text{SiH}_3\text{PH}_2$ .

Observed <sup>a</sup>			Calculated	Assignment and P. E. D.
Gas	Solid	Liquid		
2318 W			2322	$\nu_{10}$ , $\text{PH}_2$ antisymmetric stretch (100%), $A''$
2304 M	2287 M	2293 p M	2318	$\nu_1$ , $\text{PH}_2$ symmetric stretch (100%), $A'$
2189 M	2185 M	2178 p M	2199, 2198	$\nu_2$ , $\nu_{11}$ , $\text{SiH}_3$ antisymmetric stretch (100%)
2166 S	2153 S	2152 p S	2166	$\nu_3$ , $\text{SiH}_3$ symmetric stretch (100%), $A'$
1122 W		1130		
		1100 p VW	1093	$\nu_4$ , $\text{PH}_2$ scissor (99%), $\text{PH}_2$ wag (1%), $A'$
1060 VW	1057 VW	1065 dp W		$\nu_8 + \nu_9 = 1055$
	$\sim 940$ VW	955 VW	953	$\nu_5$ , $\text{SiH}_3$ antisymmetric deformation (78%), $\text{SiH}_3$ rock (10%), $\text{SiH}_3$ symmetric deformation (8%), $\text{PH}_2$ wag (4%), $A'$
			947	$\nu_{12}$ , $\text{SiH}_3$ antisymmetric deformation (90%), $\text{SiH}_3$ rock (10%), $A''$
$\sim 940$ W	925 W	930 p W	926	$\nu_6$ , $\text{SiH}_3$ symmetric deformation (78%), $\text{SiH}_3$ antisymmetric deformation (12%), $\text{PH}_2$ wag (6%), SiP stretch (3%), $\text{SiH}_3$ rock (1%), $A'$
	763 VW	770 dp VW	745	$\nu_{13}$ , $\text{PH}_2$ twist (93%), $\text{SiH}_3$ rock (7%), $A''$
722 VW	$\sim 720$ VW	725 VW	736	$\nu_7$ , $\text{PH}_2$ wag (84%), $\text{SiH}_3$ rock (16%), $A'$
602 VW	597 VW	600 VW	597	$\nu_8$ , $\text{SiH}_3$ rock (88%), $\text{PH}_2$ wag (6%), $\text{SiH}_3$ antisymmetric deformation (6%), $A'$
602 VW	597 VW	600 VW	595	$\nu_{14}$ , $\text{SiH}_3$ rock (85%), $\text{PH}_2$ twist (7%), $\text{SiH}_3$ antisymmetric deformation (8%), $A''$
$\sim 480$ W	487 W	500 p W		

Table I. (continued)

Observed			Calculated	Assignment and P. E. D.
Gas	Solid	Liquid		
452 M	445 M	455 p M	458	$\nu_9$ , SiP stretch (96%), $\text{PH}_2$ wag (2%), symmetric deformation (2%), $A'$
	432 W	440 p W		
393 VW	390 W	395 p W		
361 W	340 W	355 p W		
168 <sup>b</sup>			161	$\nu_{16}$ , torsion, $A''$

<sup>a</sup> S, M, W, V, p, and dp denote strong, medium, weak, very, polarized, and depolarized, respectively.

<sup>b</sup> Calculated from the barrier given in Table V.

Table II Observed and calculated gas Raman frequencies ( $\text{cm}^{-1}$ ) of  $\text{SiH}_3\text{PD}_2$ .

<u>Observed<sup>a</sup></u>	<u>Calculated</u>	<u>Assignment and P.E.D.</u>
2226		
2198 p S	2199	$\nu_2$ , $\text{SiH}_3$ antisymmetric stretch (100%), $A'$
2198	2198	$\nu_{11}$ , $\text{SiH}_3$ antisymmetric stretch (100%), $A''$
2186 p S	2167	$\nu_3$ , $\text{SiH}_3$ symmetric stretch (100%), $A'$
2150 W		
1612 W	1670	PDH impurity ?
1597 WM	1665	$\nu_{10}$ , $\text{PD}_2$ antisymmetric stretch (100%), $A''$
1587 M		$\nu_1$ , $\text{PD}_2$ symmetric stretch (100%), $A'$
~940 VW	950	$\nu_5$ , $\text{SiH}_3$ antisymmetric deformation (89%) $\text{SiH}_3$ rock (11%), $A'$
~940 VW	947	$\nu_{12}$ , $\text{SiH}_3$ antisymmetric deformation (90%) $\text{SiH}_3$ rock (10%), $A''$
~927 VW	917	$\nu_6$ , $\text{SiH}_3$ symmetric deformation (94%) PSi stretch (4%) $\text{SiH}_3$ antisymmetric deformation (2%), $A'$
810 VW	784	$\nu_4$ , $\text{PD}_2$ scissor (99%), $A'$
657 VW	511	$\nu_{13}$ , $\text{PD}_2$ twist (85%), $\text{SiH}_3$ rock (15%), $A''$
605 VW	622	$\nu_{14}$ , $\text{SiH}_3$ rock (89%) $\text{SiH}_3$ antisymmetric deformation (11%), $A''$
605 W	613	$\nu_8$ , $\text{SiH}_3$ rock (76%) $\text{SiH}_3$ antisymmetric deformation (11%) $\text{PD}_2$ wag (11%), PSi stretch (2%), $A'$
552 VW	556	$\nu_7$ , $\text{PD}_2$ wag (64%), $\text{SiH}_3$ rock (20%) PSi stretch (16%), $A'$
498 VW		?
427 p M	435	$\nu_9$ , PSi stretch (78%), $\text{PD}_2$ wag (22%), $A'$
143 <sup>b</sup>	149	$\nu_{15}$ $\text{SiH}_3$ torsion (100%), $A''$

<sup>a</sup> For abbreviations, see Table I.

<sup>b</sup> Calculated from the barrier given in Table V.

Table III. Observed and Calculated vibrational frequencies ( $\text{cm}^{-1}$ ) of  $\text{SiD}_3\text{PD}_2$ .

<u>Observed<sup>a</sup></u>	<u>Calculated</u>	<u>Assignment and P. E. D.</u>
1681	1671	$\nu_{10}$ , $\text{PH}_2$ antisymmetric stretch (100%), $A''$ .
1681	1665	$\nu_1$ , $\text{PH}_2$ symmetric stretch (100%), $A'$
1588	1591	$\nu_2$ , $\text{SiD}_3$ antisymmetric stretch (100%), $A'$
1588	1588	$\nu_{11}$ , $\text{SiD}_3$ antisymmetric stretch (100%), $A''$
775	785	$\nu_4$ , $\text{PD}_2$ scissor (100%), $A'$
702	710	$\nu_6$ , $\text{SiD}_3$ symmetric deformation (69%) PSi stretch (15%), $\text{PD}_2$ wag (10%), $\text{SiD}_3$ antisymmetric deformation (4%), $\text{PD}_2$ scissor (1%), $\text{SiD}_3$ symmetric stretch (1%).
673	676	$\nu_5$ , $\text{SiD}_3$ antisymmetric deformation (86%), $\text{SiD}_3$ rock (8%), $\text{SiD}_3$ symmetric deformation (6%), $A'$
682	675	$\nu_{12}$ , $\text{SiD}_3$ antisymmetric deformation (92%), $\text{SiD}_3$ rock (8%), $A''$
545	545	$\nu_7$ , $\text{PD}_2$ wag (69%), $\text{SiD}_3$ symmetric deformation (23%), PSi stretch (5%), $\text{SiD}_3$ antisymmetric deformation (2%), $A'$
	543	$\nu_{13}$ , $\text{PD}_2$ twist (86%), $\text{SiD}_3$ rock (13%), $\text{SiD}_3$ antisymmetric deformation (1%), $A''$
450	447	$\nu_8$ , $\text{SiD}_3$ rock (89%), $\text{SiD}_3$ antisymmetric deformation (7%), $\text{PD}_2$ wag (4%), $A'$
450	436	$\nu_{14}$ , $\text{SiD}_3$ rock (76%), $\text{PD}_2$ twist (17%), $\text{SiD}_3$ antisymmetric deformation (7%), $A''$ .
425	421	$\nu_9$ , PSi Stretch (80%), $\text{PD}_2$ wag (14%), $\text{SiD}_3$ symmetric deformation (5%), $\text{SiD}_3$ rock (1%), $A'$ .
	131	$\nu_{15}$ , torsion (100%), $A''$

<sup>a</sup> From ref. 5.

Table IV. Values and descriptions of the VFF force constants of silylphosphine.

<u>Force constant</u>	<u>Value (mdynes/Å°)<sup>a</sup></u>	<u>Description</u>
$K_R$	$2.04 \pm 0.07$	Si-P stretch
$K_r$	$3.10 \pm 0.02$	P-H stretch
$K_\ell$	$2.74 \pm 0.01$	Si-H stretch
$H_\gamma$	$0.68 \pm 0.01$	H-P-H bend
$H_\phi$	$0.62 \pm 0.01$	Si-P-H bend
$H_\beta$	$0.53 \pm 0.01$	P-Si-H bend
$H_\alpha$	$0.44 \pm 0.01$	H-Si-H bend
$H_\tau$	$0.004 \pm 0.01$	torsion
$F_{\beta\phi}$	$0.09 \pm 0.01$	PSiH bend/SiPH bend ( $\sim$ cis)
$F'_{\beta\phi}$	$0.04 \pm 0.02$	PSiH bend/SiPH bend ( $\sim$ gauche)
$F_{\ell\beta}$	$0.14 \pm 0.10$	SiH stretch/PSiH bend
$F_{\gamma\phi}$	$0.03 \pm 0.03$	P-H stretch/SiPH bend

<sup>a</sup> All bending coordinates are weighted by 1Å.

Table V. Rotational Transitions (MHz) of the "A" lines of  
Silylphosphine-d<sub>2</sub> (SiH<sub>3</sub>PD<sub>2</sub>) in the Ground  
Vibrational State.

Transition	$\nu(\text{obs.})$	$\Delta\nu(\text{obs.}-\text{calc.})$
b-type		
$1_{11} \leftarrow 1_{01}$	32273.35	-0.01
$2_{12} \leftarrow 2_{02}$	32216.46	0.02
$3_{13} \leftarrow 3_{03}$	32131.20	0.01
$4_{14} \leftarrow 4_{04}$	32017.80	-0.01
$5_{15} \leftarrow 5_{05}$	31876.55	0.05
$6_{16} \leftarrow 6_{06}$	31707.53	-0.02
a-type		
$3_{13} \leftarrow 2_{12}$	31637.74	0.10
$3_{12} \leftarrow 2_{11}$	31808.66	0.06
$3_{22} \leftarrow 2_{21}$	31723.04	-0.15

Table VI. Effective Rotational Constants (MHz) and Moments of Inertia ( $\text{u}\cdot\text{\AA}^2$ )<sup>a</sup> of  $\text{SiH}_3\text{PD}_2$  in the Ground Vibrational State.

---

$A = 37589.06 \pm 0.11$	$I_a = 13.44516$
$B = 5315.70 \pm 0.02$	$I_b = 95.0752$
$C = 5258.70 \pm 0.02$	$I_c = 96.1057$
$\kappa = -0.996474$	

<sup>a</sup>Conversion factor:  $505391 \text{ MHz}\cdot\text{u}\cdot\text{\AA}^2$ .

Table VII. Stark Coefficients [ $\text{MHz}\cdot\text{cm}^2/(\text{k}\cdot\text{volt})^2$ ] and Dipole Moment Components (Debye) of  $\text{SiH}_3\text{PD}_2$ .

Transition	$ M $	$\Delta\nu/E^2$	
		Observed	Calculated <sup>a</sup>
$3_{13} \leftarrow 3_{03}$	3	-0.402	-0.401
$4_{14} \leftarrow 4_{04}$	4	1.054	1.052
$5_{15} \leftarrow 5_{05}$	4	0.874	0.877
$5_{15} \leftarrow 5_{05}$	5	1.583	1.583

$$\mu_a = 0.22 \pm 0.01$$

$$\mu_b = 0.00 \text{ (by symmetry)}$$

$$\mu_c = 0.56 \pm 0.01$$

$$\mu_T = 0.60 \pm 0.01$$

<sup>a</sup>Calculated from the dipole moment components listed in this table.



Table VIII. Internal Rotation Splittings (MHz) and Parameters of  $\text{SiH}_3\text{PD}_2$ .

Transition	$\nu_E - \nu_A$	$V_3$ (cal/mole)
$1_{11} \leftrightarrow 1_{01}$	-26.12	1514
$2_{12} \leftrightarrow 2_{02}$	-21.47	1511
$3_{13} \leftrightarrow 3_{03}$	-20.09	1509
$4_{14} \leftrightarrow 4_{04}$	-19.43	1510
$5_{15} \leftrightarrow 5_{05}$	-19.00	1511
$6_{16} \leftrightarrow 6_{06}$	-19.02	1508
$3_{13} \leftrightarrow 2_{12}$	1.38	1522
$3_{12} \leftrightarrow 2_{11}$	-1.39	1522
$6_{06} \leftrightarrow 5_{14}$	18.11	1506
$6_{16} \leftrightarrow 5_{24}$	68.86	1526
$I_\alpha = 5.928 \text{ u}\cdot\text{\AA}^2$		$\alpha = 0.4408$
$F = 152.4 \text{ kHz}$		$\beta = 0$
$\bar{V}_3 = 1512 \text{ kcal/mole}$		$\gamma = 0.0011$

## FIGURE CAPTIONS

Figure 1. (A) Raman spectrum of solid  $\text{SiH}_3\text{PH}_2$ , (B) Raman Spectrum of liquid  $\text{SiH}_3\text{PH}_2$ , (C) Raman spectrum of gaseous  $\text{SiH}_3\text{PH}_2$ , (D) Raman spectrum of gaseous  $\text{SiH}_3\text{PD}_2$ .

ORIGINAL PAGE IS  
OF POOR QUALITY

